Structure and magnetic properties of $(Fe_{0.5}Co_{0.5})_{88}Zr_7B_4Cu_1$ nanocrystalline alloys

M. A. Willard,[a] D. E. Laughlin, and M. E. McHenry
Department of Materials Science and Engineering, Carnegie Mellon University, Pittsburgh, Pennsylvania 15213-3890

D. Thoma and K. Sickafus
Los Alamos National Laboratory, Los Alamos, New Mexico 87545

J. O. Cross and V. G. Harris
Naval Research Laboratory, Washington, D.C. 20375-5000

The development of $Fe_{73.5}Si_{13.5}B_9Nb_3Cu_1$ (FINEMET) by Yoshizawa *et al.* and $Fe_{88}Zr_7B_4Cu_1$ (NANOPERM) by Inoue *et al.* have shown that nanocrystalline microstructures can play an important role in the production of materials with outstanding soft magnetic properties. The FINEMET and NANOPERM materials rely on nanocrystalline α-Fe_3Si and α-Fe, respectively, for their soft magnetic properties. The magnetic properties of a new class of nanocrystalline magnets are described herein. These alloys with a composition of (Fe,Co)–M–B–Cu (where M=Zr and Hf) are based on the α- and α'-FeCo phases, have been named HITPERM magnets, and offer large magnetic inductions to elevated temperatures. This report focuses on thermomagnetic properties, alternating current (ac) magnetic response, and unambiguous evidence of α'-FeCo as the nanocrystalline ferromagnetic phase, as supported by synchrotron x-ray diffraction. Synchrotron data have distinguished between the HITPERM alloy, with nanocrystallites having a B2 structure from the FINEMET alloys, with the $D0_3$ structure, and NANOPERM alloys, with the A2 structure. Thermomagnetic data shows high magnetization to persist to the $\alpha \rightarrow \gamma$ phase transformation at 980 °C. The room temperature ac permeability has been found to maintain a high value of 1800 up to a frequency of $\sim$2 kHz. The room temperature core loss has also been shown to be competitive with that of commercial high temperature alloys with a value of 1 W/g at $B_S = 10$ kG and $f = 1$ kHz. © *1998 American Institute of Physics.* [S0021-8979(98)03024-2]

I. INTRODUCTION

The demands on bulk soft magnetic materials for high temperature power applications include the development of magnets (1) capable of operating at higher temperatures and (2) possessing higher combined inductions and permeabilities. Issues important in achieving such goals include alloy chemistry, crystal structure, and the ability to tailor microstructural features. It is clear that magnets used in such soft magnetic applications must be optimized in terms of their intrinsic and extrinsic magnetic properties as well as their morphology. A key intrinsic magnetic property is the saturation induction, B_S, of the material that is determined by alloy composition. Exceptional high induction materials include Fe, Co, and Fe–Co alloys. The extrinsic property of interest is the magnetic permeability, $\mu(H)$, which is the magnetic response function in applied field. The magnetic permeability is determined by a combination of chemistry, structure, and morphology (sample shape or grain shape in granular materials). In particular, alloys with small magnetocrystalline anisotropies and magnetostrictive coefficients give rise to particularly soft magnetic materials.

Choice of a soft magnetic material for high temperature magnetic applications (such as rotors in electric aircraft) will be guided by developments in the field of soft magnetic materials. Conventional methods of developing these materials has relied on the reduction of coercivity by increasing the grain size of the magnetic phase, thus reducing the pinning of domain walls at grain boundaries. Another philosophy is to use nanocrystalline materials, where the grains are much smaller than the domain wall width parameter, so that the magnetic anisotropy is averaged over many grains and orientations.[1] As a result, in nanocrystalline alloys, the coercivity can be significantly reduced and alternating current (ac) permeability increased as compared with conventional alloys having much larger grains.

Amorphous and nanocrystalline magnetic materials, in terms of combined induction and permeabilities, are now competitive with Si–Fe bulk alloys, and the above mentioned Fe–Co alloys. Conventional Fe–Co alloys are particularly attractive because of their large inductions, while their permeabilities are smaller than those of amorphous and nanocrystalline alloys and Si steels. In Fig. 1, Co-based amorphous alloys, Fe-based amorphous alloys, nanocrystalline Fe–Si–B–Nb–Cu (Ref. 2) alloys and Fe–M–B–Cu (Refs. 3,4) (M=Zr, Nb, Hf,···) nanocrystalline alloys have all been optimized to achieve small magnetostrictive coefficients and concomitant large permeabilities.

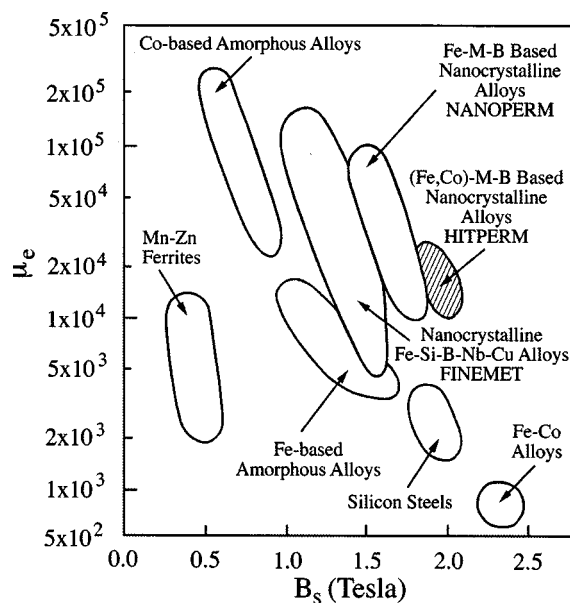[a]Electronic mail: mw4t+@andrew.cmu.edu

FIG. 1. Relationship of the permeability to magnetic induction in nanocrystalline, amorphous and conventional crystalline soft magnetic alloys (adapted from Inoue) (see Ref. 6).

FIG. 2. Differential thermal analysis showing two distinct crystallization peaks, at $T_{x1} = 510\,°C$ and $T_{x2} = 700\,°C$. These peaks correspond to the crystallization of α'-FeCo and $(Fe,Co)_3Zr$, respectively.

Premiere nanocrystalline soft magnetic materials based on $Fe_{73.5}Si_{13.5}B_9Nb_3Cu_1$ and $Fe_{88}M_7B_4Cu_1$ have been patented under the tradenames FINEMETS[2] and NANOPERM,[3,4] respectively. In FINEMET alloys, α-Fe_3Si nanocrystalline grains often with partial ordering in a DO_3 crystal structure are observed, in NANOPERM, α-Fe nanocrystals with a body centered cubic (BCC) (A2) structure are formed. We have investigated (Fe,Co)–Zr–B–Cu produced by rapid solidification processing followed by primary crystallization. In these and similar alloys with the composition (Fe,Co)–M–B–Cu, where M=Zr, Nb, Hf, etc., which we call HITPERM. Nanocrystalline α'-FeCo grains (B2 structure) are formed exhibiting significantly improved high temperature magnetic induction than in the former two systems. In this work we describe the synthesis, structure, and magnetic properties of $(Fe,Co)_{88}Zr_7B_4Cu$ alloys which we propose as excellent candidates for high temperature soft magnetic materials.

II. EXPERIMENTAL PROCEDURES

Samples of the composition $Fe_{44}Co_{44}Zr_7B_4Cu_1$ were prepared by arc melting of electrolytic Fe (99.9% pure with low C), Co (99.9% pure), Zr (99.9% pure), Fe_3B (90.75% metals basis), and Cu (99.99% pure) in an argon atmosphere. Amorphous ribbons were then produced from the ingots using a single wheel melt spinning technique. The process used for melt spinning began with remelting of the arc-melted ingot in a boron nitride crucible with an argon atmosphere. A small positive pressure of argon was then used to quench the molten alloy onto a Cu–Be wheel. The wheel speed was 35 m/s and the ribbons obtained by this process were approximately 1 mm in width and 20–50 μm in thickness. After obtaining the as spun ribbons from the melt spinning procedure, they were isothermally annealed ($510\,°C < T_{ann}$

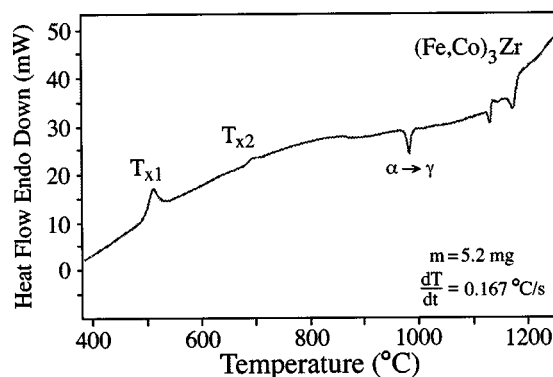$< 700\,°C$) in an inert (Ar) atmosphere for 1 h followed by water quenching resulting in the nanocrystalline microstructure.

Differential thermal analysis (DTA) was used to examine the crystallization temperatures of an as-cast ribbon. A scanning rate of $0.167\,°C/s$ was used at temperatures between 400 and 1200 °C. The structure of the ribbon was examined by x-ray diffraction using a Scintag XDS 2000 diffractometer, and Cu $K\alpha$ radiation. Synchrotron x-ray diffraction experiments were performed at the National Synchrotron Light Source to identify the superlattice reflections which are signatures of the ordered α'-FeCo phase. X-rays with an energy of 7112 eV or equivalently a wavelength of 1.748 Å were used for the synchrotron x-ray experiments. This wavelength was chosen to take advantage of the anomalous scattering just above the Fe K edge.

The vibrating sample magnetometer was used to measure the magnetization as a function of temperature of the as quenched and annealed materials from room temperature to 1000 °C, in a field of 500 Oe, and with a heating rate of 2 °C/min. A Walker ac permeameter was used to measure the room temperature permeability and coercivity of toroidal samples. The as-spun ribbons were prepared for permeability measurement by winding them into laminated toroids followed by the standard isothermal anneal for nanocrystallization prior to measurement of ac properties.

III. RESULTS AND DISCUSSION

The material described in this study has been found to have large magnetizations to high temperatures, large room temperature ac permeability, and core loss at room temperature competitive with that of conventional alloys. This is due in part to the formation of the nanocrystalline grains with the ordered α'-FeCo structure. In the following we discuss the results of structural determination and thermodynamic analysis, intrinsic magnetic properties, and extrinsic (technical) magnetic properties.
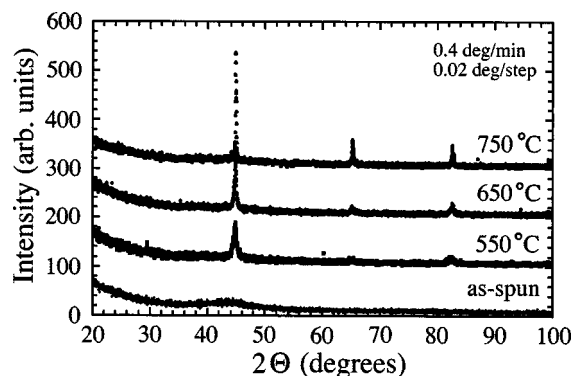
FIG. 3. Conventional XRD experiments on the as-cast alloy and the alloy annealed at three different temperatures for 1 h, with a water quench. The as-spun ribbon is seen to be amorphous, and the annealed samples are a BCC-derivative phase (either α- or α'-FeCo) (a=2.858 Å).

FIG. 4. Synchrotron XRD ($E=7112$ eV and $\lambda=1.748$ Å) experiment which shows a (100) superlattice reflection, thus distinguishing the ordered α'-FeCo phase from the disordered α-FeCo phase.

A. Structural determination and thermodynamic analysis

DTA has been used to determine the temperatures of crystallization for this alloy. Figure 2 shows two distinct crystallization events. These are labeled T_{x1} at 510 °C and T_{x2} at 700 °C. These peaks correspond to the primary crystallization of α'-FeCo and secondary crystallization of $(\text{Fe,Co})_3\text{Zr}$, respectively. At temperatures higher than T_{x2}, additional crystallization events associated with the intergranular amorphous phase are also possible leading to the formation of refractory boride precipitates, for example. At this time we do not have firm structural evidence for the boride crystallization, but evidence for additional crystallization events is presented in $M(T)$ data below. In order to take advantage of the soft magnetic properties of the magnetic α'-FeCo nanocrystallites it is important to have as great a difference as possible between T_{x1} and T_{x2}. This allows for the crystallization of the α'-FeCo phase without the crystallization of nonferromagnetic phases which magnetically harden the materials. The addition of small amounts of Cu to the alloy is commonly thought to depress T_{x1},[5,6] and to provide Cu clusters in incipient crystallization which act as nucleation sites for the primary nanocrystals. The addition of the elements Zr and B allow for better glass formation during melt spinning, which is the essential precursor for the formation of the nanocrystals.

To confirm the formation of the phases at each of the crystallization temperatures, x-ray diffraction (XRD) experiments were conducted. From the conventional XRD results seen in Fig. 3, the as-spun ribbon is amorphous, and the formation of either the α-FeCo or α'-FeCo phases occurs at annealing temperatures above T_{x1}. Closer inspection of the sample annealed at 750 °C, just above T_{x2}, shows the formation of a small amount of $(\text{Fe,Co})_3\text{Zr}$ phase.

Ambiguity in distinguishing between the α-FeCo and α'-FeCo phases above T_{x1} in conventional x-ray analysis, is due to the similarity of the atomic scattering factors of Fe and Co. This makes the observation of the superlattice reflections in conventional XRD quite difficult, since the intensity of the superlattice reflections is proportional to the square of the differences of the two atomic scattering factors.
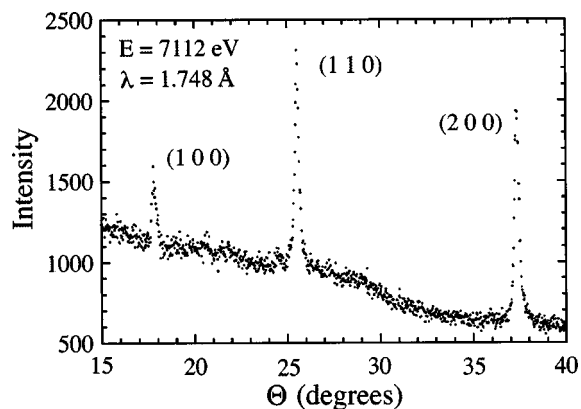
However, by using the intense beam of the synchrotron x-ray source and choosing the radiation wavelength to take advantage of anomalous scattering we have increased the difference in atomic scattering factors allowing for observation of superlattice reflections. In Fig. 4, the synchrotron XRD pattern shows that the atomically ordered α'-FeCo phase has indeed been formed by the presence of the (100) superlattice reflection. This sample was annealed at 550 °C which is below the temperature of the bulk order–disorder phase transformation, so that in equilibrium we should expect the ordered phase.

B. Intrinsic magnetic properties

Figure 5 shows the magnetization as a function of temperature for two alloys, one of the NANOPERM composition and the other of the HITPERM composition. Initially, both of the samples are amorphous and as the samples are heated, the crystallization of the amorphous phase becomes apparent in each alloy by an increase in magnetization. The lower curve, for the NANOPERM material, shows the Curie temperature of the amorphous alloy to be just above room temperature. The magnetic phase transition is followed by primary crystallization at $T_{x1} \sim 500$ °C. This is followed by
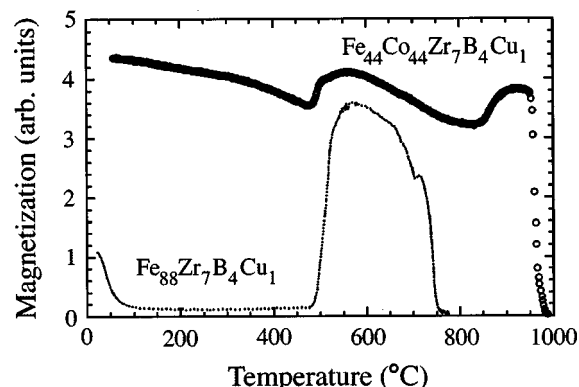
FIG. 5. Thermomagnetic data showing the alloys of the HITPERM (large circles) and NANOPERM alloy compositions (small circles). The HITPERM maintains a high magnetization to very high temperatures, which makes it an excellent candidate for high temperature applications.
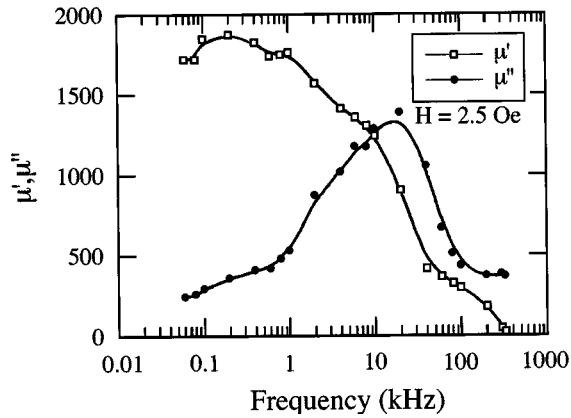
FIG. 6. AC permeability is shown as a function of frequency. The sample was prepared in a laminated toroidal geometry, annealed at 600 °C and measured with a field amplitude of 2.5 Oe. Notice the loss peaks at about 20 kHz and a maximum permeability of 1800.

secondary crystallization and then finally the Curie temperature for the α-Fe phase at $\sim$770 °C. The upper curve for HITPERM, shows that the magnetization decreases monotonically until $\sim$400 °C as the amorphous phase approaches its Curie temperature. Near 500 °C structural relaxation and crystallization of the α'-FeCo phase occurs resulting in larger magnetization due to the higher Curie temperature of the α'-FeCo phase. The crystallization temperature is therefore well below the Curie temperature of the amorphous phase, so that the magnetization of the amorphous phase is only partially suppressed prior to crystallization. At a temperature corresponding to the $\alpha \rightarrow \gamma$ phase transition (980 °C), the material abruptly loses its magnetization consistent with the paramagnetic response of the γ phase.

At approximately 700 °C in the NANOPERM alloy and at $\sim$900 °C in the HITPERM alloy, anomalous peaks in the magnetization are seen. We do not have structural data to confirm our expectation, however, it seems reasonable that at a high enough temperature, a reaction where the remaining amorphous phase (which is rich in Zr and B) could be converted in part to ZrB_2. This would further increase the volume fraction of α-FeCo and thus the magnetization.

C. Extrinsic magnetic properties

For permeability measurements, the sample was prepared as a laminate in a toroidal geometry, and then annealed at 600 °C to promote primary crystallization. AC permeability measurements were performed with a field amplitude of 2.5 Oe. Figure 6 illustrates the frequency dependence of the real and imaginary components of the complex permeability, μ' and μ'', respectively. μ'' reflects to the power loss due to eddy currents and hysteretic response. The maximum permeability for this material was determined to be about 1800. $\mu''(f)$ peaks at the frequency $\sim$20 kHz. The ac permeability at room temperature of the HITPERM alloy has been compared to a commercial alloy with nominal composition $(FeCo)_{98}V_2$, called HIPERCO-50 alloy. Table I shows a summary of the results of these experiments.

The importance of the two-phase microstructure in nanocrystalline alloys has been discussed in detail for FINEMET alloys.[7–11] The nature of the nanocrystal–amorphous–nanocrystal coupling is of paramount importance to the properties of these materials. This coupling depends both on the size of the nanocrystallites and more importantly on the amount, chemistry, thickness and in particular the Curie temperature of the intervening amorphous phase. It is imperative for the ferromagnetic grains to be strongly exchange coupled to maintain good soft magnetic properties. If the exchange coupling is disrupted then the coercivity will increase, the permeability will decrease, and the Herzer model is no longer applicable.[11]

Slawska-Waniewska *et al.*[7] have observed T-dependent magnetic response in nanocrystallized FINEMET materials. They concluded that for sufficiently small nanocrystals with enough intergranular material between them to diminish or destroy the coupling between particles that superparamagnetic response is observed. Skorvanek and O'Handley[8] have studied magnetic interactions between nanoparticles in FINEMET above the Curie temperature of the intergranular amorphous phase. They show that the magnetic interactions increase with increasing nanocrystalline volume fraction. These interactions tend to suppress superparamagnetic fluctuations. They observe a peak $H_C(T)$ near the Curie temperature of the amorphous phase.

An elegant phenomenological model has been developed by Hernando, *et al.*,[9,10] which also describes the differences

TABLE I. Comparison of ac permeability characteristics of NANOPERM, HITPERM, and HIPERCO-50 at room temperature.

Sample	Constant	HIPERCO-50	$Fe_{88}Zr_7B_4Cu_1$ annealed at 600 °C	$Fe_{44}Co_{44}Zr_7B_4Cu_1$ annealed at 600 °C
P_{cm}-B	$f = 0.4$ kHz	0.01 W/g 10 kG	0.003 W/g 10 kG	0.02 W/g ⋯
P_{cm}-B	$f = 10$ kHz	1.8 W/g 15 kG	0.8 W/g 15 kG	1 W/g 10 kG
$f(\mu''$ peak$)$	$H = 1$ Oe	1 kHz	20 kHz	2 kHz
$f(\mu''$ peak$)$	$H = 2.5$ Oe		60 kHz	20 kHz
H_c	$H_m = 10$ Oe	4 Oe (10 kHz)	0.7 Oe (10 kHz) 2 Oe (50 kHz)	2 Oe (4 kHz) 2.2 Oe (10 kHz)

in soft magnetic properties (K_{eff}) from the Herzer one-phase model near the Curie temperature of the amorphous phase, T_c^{am} where the nanoparticles decouple. For these reasons FINEMET alloys (and probably NANOPERM alloys) are not suitable for use at high temperatures (above the T_c^{am} transition at $\sim350\,°C$).

While it is difficult to get an accurate fit of the $M(T)$ of the HITPERM amorphous phase because the order parameter has been suppressed by only $\sim25\%$ at the temperature of primary crystallization, T_{x1}, even the most conservative estimate would place the Curie temperature of the amorphous phase well above $600\,°C$. With the amorphous phase remaining ferromagnetic, the strong exchange coupling should not be disrupted at much higher temperatures than for the Fe-based nanocrystalline magnets. For this reason, we expect that these alloys should maintain good soft magnetic properties to high temperatures, where other Fe-based alloys cannot. We will report on high temperature ac magnetic measurements in the future.

We are currently modeling the ac losses using equations of motion for a domain wall in a viscous medium. The high peak frequency is thought to be reflective of the higher resistivity in the nanocrystalline materials than that of the conventional alloys. The resistivity is a significant term in eddy current related damping of domain wall motion.

IV. CONCLUSIONS

New nanocrystalline soft magnetic material with the α'-FeCo phase (B2 structure) are reported. These have been shown to have excellent magnetic properties to high frequencies and temperatures. Both the improved high temperature properties of the α'-FeCo nanocrystalline phase and of the intergranular matrix material (T_c^{am}) suggest that this material will be an important candidate for high temperature aircraft power applications.

[1] The domain wall width parameter is the equivalent of Herzer's magnetic exchange length, G. Herzer, IEEE Trans. Magn. **26**, 1397 (1990); J. Magn. Magn. Mater. **112**, 258 (1992).

[2] Y. Yoshizawa, S. Oguma, and K. Yamaguchi, J. Appl. Phys. **64**, 6044 (1988).

[3] K. Suzuki, A. Makino, N. Kataoka, A. Inoue, and T. Masumoto, Mater. Trans., JIM **32**, 93 (1991).

[4] A. Makino, T. Hatanai, Y. Naitoh, T. Bitoh, A. Inoue, and T. Masumoto, IEEE Trans. Magn. **33**, 3793 (1997).

[5] K. Suzuki, A. Makino, A. Inoue, and T. Masumoto, J. Appl. Phys. **70**, 6232 (1991).

[6] A. Makino, A. Inoue, and T. Masumoto, Mater. Trans., JIM **36**, 924 (1995).

[7] A. Slawska-Waniewska, M. Gutowski, H. K. Lachowicz, T. Kulik, and H. Matyja, Phys. Rev. B **46**, 14594 (1992).

[8] I. Skorvanek and R. C. O'Handley, J. Magn. Magn. Mater. **140–144**, 467 (1995).

[9] A. Hernando, M. Vázquez, T. Kulik, and C. Prados, Phys. Rev. B **51**, 3581 (1995).

[10] A. Hernando and T. Kulik, Phys. Rev. B **49**, 7064 (1994).

[11] G. Herzer, Phys. Scr. **T49**, 307 (1993).